



# Epidermal growth factor receptor mutation accelerates radiographic progression in lung adenocarcinoma presented as a solitary ground-glass opacity

Qijue Lu<sup>#</sup>, Ye Ma<sup>#</sup>, Zhao An<sup>#</sup>, Tiejun Zhao, Zhiyun Xu, Hezhong Chen

Department of Cardiothoracic Surgery, Changhai Hospital, Second Military Medical University, Shanghai 200433, China

**Contributions:** (I) Conception and design: H Chen, Z Xu; (II) Administrative support: None; (III) Provision of study materials or patients: Z An, Y Ma; (IV) Collection and assembly of data: Q Lu, Z An; (V) Data analysis and interpretation: Q Lu, Y Ma, TJ Zhao; (VI) Manuscript writing: All authors; (VII) Final approval of manuscript: All authors.

<sup>#</sup>These authors contributed equally to this work.

**Correspondence to:** Zhiyun Xu; Hezhong Chen. Department of Cardiothoracic Surgery, Changhai Hospital, Second Military Medical University, Shanghai 200433, China. Email: doctorhsd@sina.com; drchenhz@sina.com.

**Background:** We aimed to investigate the impact of epidermal growth factor receptor (EGFR) mutation in the progression of lung adenocarcinoma presented as a solitary ground-glass opacity (GGO) by retrospectively evaluating the correlation between EGFR mutation status and the radiographic features.

**Methods:** One hundred fifty-six cases of lung adenocarcinoma presented as a solitary GGO were enrolled between 2013 and 2015. Chest CT scans were performed 3 times (1st  $\geq 3$  months, 2nd  $\leq 1$  week preoperatively and 3rd  $\geq 3$  months postoperatively) in each patient. The diameter and volume of every lesion was measured by semiautomated algorithm. EGFR mutation hotspots from exons 18, 19 and 21 were detected by real-time PCR.

**Results:** In the 156 patients who were enrolled in our study, tumors in 75 patients (48.1%) were pathologically diagnosed with EGFR-mutant, with 1, 29 and 45 cases harboring tumors with mutation in exon 18, 19 and 21, respectively. EGFR mutation occurred more frequently in women ( $P=0.005$ ) and non-smokers ( $P=0.019$ ). Comparison between the 1st and 2nd preoperative CT scans showed that 28 (37.3%) of 75 patients with EGFR mutations had an over 50% increment of tumor size and 38 (52.0%) displayed a growth of solid component. On the other hand, we found only 9 (11.1%) and 14 (17.3%) in 81 lesions without EGFR mutation had a distinct volume growth and component solidification, respectively, which is significantly less than that in EGFR mutation lesions ( $P<0.001$ ). Further, in the postoperative CT scan, recurrent GGOs or nodes were identified in 6 (8%) EGFR-mutant patients and 6 (7.4%) in wild-type patients ( $P=0.89$ ), which indicates no overt statistically difference. At last, we found that EGFR amplification is more frequent as GGO volume percentage decreases and diameter increases.

**Conclusions:** We found GGOs with EGFR mutation grew faster in volume and solidified more quickly in component than wild-type GGOs. Moreover, in the follow-up after surgery, patients in the EGFR mutation group and EGFR wild-type group showed no significant difference in the imaging evolution.

**Keywords:** Epidermal growth factor receptor (EGFR); ground-glass opacity (GGO); lung adenocarcinoma

Submitted Feb 26, 2018. Accepted for publication Sep 11, 2018.

doi: 10.21037/jtd.2018.10.19

**View this article at:** <http://dx.doi.org/10.21037/jtd.2018.10.19>

## Introduction

With increased early detection in lung cancer screening due to the recently widespread availability of low-dose CT, ground-glass opacity (GGO) has become a major concern (1). According to the 2011 International Association for the Study of Lung Cancer/American Thoracic Society/European Respiratory Society (IASLC/ATS/ERS) classification system, surgically resected GGO lesions were pathologically suggestive of neoplastic conditions including atypical adenomatous hyperplasia (AAH), adenocarcinoma *in situ* (AIS), minimally invasive adenocarcinoma (MIA) and invasive adenocarcinoma (IA) (2-4). Several retrospective studies have demonstrated that a high GGO proportion in adenocarcinoma could be a sensitive predictor of favorable prognosis, particularly when GGO in peripheral adenocarcinoma is less than 3 cm in diameter (5-7).

Somatic mutations in the tyrosine kinase domain (exon 18-21) of the epidermal growth factor receptor (EGFR) are closely correlated with the good clinical response to EGFR tyrosine kinase inhibitors (TKIs) such as Gefitinib and Erlotinib (8,9). Specifically, a short in-frame deletion in exon 19 and a specific point mutation (L858R) in exon 21 account for approximately 90% of all activating mutations (10). Furthermore, EGFR mutation has been reported to be strongly associated with Asian ethnicity, female gender, nonsmoking status and adenocarcinoma histologic findings (11,12). Due to the predictive value of TKIs, molecular testing for mutant EGFR in lung adenocarcinoma has been used in routine clinical practices to guide treatment decisions (9).

To our knowledge, only a few reports have examined the association between lung adenocarcinoma presented as GGO and a non-significantly high frequency of EGFR mutation (13). Additionally, the relationship between clinical behaviors of pulmonary nodules with GGO and the EGFR mutation status remains largely unknown. Therefore, our study sought to identify the potential impacts of mutant EGFR on growth, consolidation and recurrence of GGOs.

## Methods

### Patients

We retrospectively reviewed a total of 1,603 consecutive patients who were pathologically diagnosed as lung adenocarcinoma and underwent lung wedge resection or lobectomy in the Changhai Hospital of the Second

Military Medical University between January 2013 and December 2015. The inclusion criteria were as follows: (I) the initial CT images showed a solitary GGO as their only radiographic characteristics; (II) CT chest scans were performed on each patient at least 3 times ( $\geq 3$  months before surgery for the 1st time,  $\leq 1$  week before surgery for the 2nd time and  $\geq 3$  months after surgery for the 3rd time); (III) the pathological reports of the surgically resected specimen for EGFR mutation test were available; (IV) neither an anti-cancer treatment nor a positron emission tomography-computerized tomography (PET-CT) scan was performed prior to the surgical resection or during the CT follow-up period. Finally, 156 cases that met these criteria were identified for this study. All the enrolled patients received wedge resection, segmentectomy or lobectomy. The surgery maintained the following indications: a maximum diameter of a GGO was larger than 1 cm, the GGO in the 2nd CT had grown when compared to the 1st CT, and the ratio of solid component inside a GGO was identified increased. Information about patient's age, gender, and smoking status were obtained from clinical records. The TNM classification was determined according to the Union for International Cancer Control and the American Joint Committee on Cancer staging system, 7th edition (14). Pathological subtypes were classified by two experienced pathologists who were blinded to the CT findings following the IASLC/ATS/ERS guidelines (15). GGO patterns were discerned by 2 independent radiologists.

### CT analysis and follow-ups

The maximum diameter was used when assessing GGOs growth by performing low-dose multi-slice spiral CT (16). Two experienced radiologists interpreted CT images. By using the presence or absence of air bronchogram as morphologic characteristics, we consequently classified these lesions as bubblelike lucency, cavitation, lobulated border, notch and round. Bubblelike lucency was seen as small spots of air attenuation within lesions. A lobulated border was recognized when the surface of a lesion showed a shallow, wavy configuration. A notch was defined as a V-shaped indentation of the border deeper than 3 mm. The round tumor was defined when the maximum and perpendicular diameter were identical without a notch. All the discrepancies were resolved by discussion until consensus was reached. Volume measurement for GGO was performed by computer. The

entire tumor mass was separated from the surrounding anatomic structures by using a semiautomated segmentation algorithm which was devised to automatically extract the bronchial and cavitory structures in the mass. A Gaussian mixture model was used to estimate the opacity distributions of the solid and GGO portions. The solid portion was segmented by using a Markov random field model according to the opacity distribution. The volumes of the entire mass and GGO portion were automatically calculated by using the computer algorithm after the segmentation and manual correction were completed. Estimated lesion volume was calculated by using the formula  $V = 4/3 \pi (d/2)^3$ , where V is the volume and d is the maximum tumor diameter (17).

According to the consolidation/tumor ratio (CTR), which was defined as the proportion of the maximum diameter of consolidation relative to the maximum tumor diameter, patients were classified into pure GGO group (CTR = 0) and mixed GGO (part-solid) group ( $0 < \text{CTR} \leq 0.5$ ) (18). All 156 patients received initial CT detections at least 3 months prior to surgery (defined as the 1st CT scan) and a solitary GGO was confirmed as the only finding in each CT scan. Both pure and mixed types were taken into account. We intentionally evaluated the latest preoperative CT examination ( $\leq 1$  week before surgery, defined as the 2nd CT scan) and made a comparison between the 1st and 2nd scans to find out potential dynamic changes. In our study, we mainly focused on increased CTR (Figure 1A,B) and enlarged volume (Figure 1 C,D) compared to the previous lesion, and the new GGOs in the same lobe or other lobes after resection of the previous one. All the patients enrolled underwent a surgical management including a wedge resection and lobectomy by VATS or thoracotomy. The growth ratio was calculated by the formula  $\text{GR} (V) = (V_2 - V_1)/V_1$ ,  $\text{GR} (d) = (d_2 - d_1)/d_1$ , where GR is growth ratio, V is volume and d is diameter.

### EGFR mutation analysis

Genomic DNA was extracted from resected tumor specimens and EGFR mutations were testified and offered by the Department of Pathology in Changhai Hospital. The ADx EGFR Mutations Detection Kit (Amoy Diagnostics, Xiamen, China), based on amplification refractory mutation system (ARMS) real-time polymerase chain reaction technology, was used to analyze the 29 EGFR mutation hotspots in exon 18, 19 and 21. The detections were carried out following the manufacturer's instructions.

### Statistical analysis

The descriptive statistics for categorical variables were reported as frequencies and percentages and continuous variables as mean  $\pm$  standard deviation. Alternations in volume and diameter between the first 2 times CT scan were analyzed by the Student *t*-test, while nominal categorical variables were compared using the (fisher)  $\chi^2$  test. All statistical analyses were performed using SPSS software (Version 18.0, Chicago, IL, USA), and P values of less than 0.05 were considered statistically significant.

### Results

We examined 1,603 consecutive patients who received a surgical resection for lung adenocarcinoma from 2013 to 2015. One hundred fifty-six patients consisting of 68 (44%) males and 88 (56%) females met our inclusion criteria and were enrolled in this study. The mean age was  $56 \pm 11$  years, ranging from 32 to 78 in females and  $58 \pm 11$  years for the 33 to 80 male group. EGFR mutation analyses had identified 75 cases with EGFR mutations and 81 cases without EGFR mutations. Mutations in exon 18, exon 19 and exon 21 were found in 1 (1%), 29 (39%) and 45 (60%) lesions, respectively. The demographic characteristics, EGFR mutation status, and pathological details are shown in Table 1. EGFR mutations were more frequently present among females (51 of 88, 58%) than among males (24 of 68, 35%) ( $P=0.005$ ) and more often in non-smokers (63 of 118, 53%) than in smokers (12 of 38, 32%) ( $P=0.019$ ). Regarding the pathological characteristics, selected patients were diagnosed as AAH/AIS ( $n=39$ ), MIA ( $n=17$ ) and IA ( $n=100$ ). The frequencies of EGFR mutation did not significantly differ among the three pathologic groups ( $P=0.515$ ).

The 1st CT scans showed that the initial maximum tumor diameter and total tumor volume of all 156 GGOs were  $1.33 \pm 0.38$  cm and  $1.53 \pm 1.32$  cm<sup>3</sup>, respectively. As presented in Table 2, the diameter and volume of the GGOs in the EGFR mutation group were  $1.34 \pm 0.36$  cm and  $1.53 \pm 1.28$  cm<sup>3</sup> while the corresponding figures in the EGFR wild-type group were  $1.31 \pm 0.40$  cm and  $1.52 \pm 1.37$  cm<sup>3</sup>. 150  $\pm$  73 days after the 1st CT scan (149  $\pm$  77 days in EGFR mutation group and 152  $\pm$  71 days in wild-type group,  $P=0.76$ ), the diameter and volume in the 2nd CT scans increased to  $1.45 \pm 0.45$  cm and  $2.08 \pm 2.07$  cm<sup>3</sup>, respectively, which were both significantly larger than their counterparts in the 1st CT scans ( $P < 0.001$ ). The tumor sizes in both

**Table 1** Demographic characteristics and EGFR mutation status in 156 patients presenting as single GGO lesion

Variable	Total	Mutation, n (%)	Wild, n (%)	$\chi^2$	P
Age (years)				0.086	0.769
≤60	98	48 (30.8)	50 (32.1)		
>60	58	27 (17.3)	31 (19.9)		
Gender				7.891	0.005
Male	68	24 (15.4)	44 (28.2)		
Female	88	51 (32.7)	37 (23.7)		
Smoking status				5.478	0.019
Smoker	38	12 (7.7)	26 (16.7)		
Non-smoker	118	63 (40.4)	55 (35.3)		
Pathological type				1.326	0.515
AAH/AIS	39	20 (12.8)	19 (12.2)		
MIA	17	10 (6.4)	7 (4.5)		
IA	100	45 (28.8)	55 (35.3)		

GGO, ground-glass opacity; EGFR, epidermal growth factor receptor; AAH, atypical adenomatous hyperplasia; AIS, adenocarcinoma in situ; MIA, minimally invasive adenocarcinoma; IA, invasive adenocarcinoma.

**Table 2** Diameter and volume of 156 GGOs between the 1st and 2nd chest CT scan in EGFR mutation group and wild-type group

Group	1st		2nd		P (d)	P (V)
	d (cm)	V (cm <sup>3</sup> )	d (cm)	V (cm <sup>3</sup> )		
Mutation	1.34±0.36	1.53±1.28	1.52±0.43	2.29±2.18	<0.001	<0.001
Wild	1.31±0.40	1.52±1.37	1.39±0.46	1.88±1.94	<0.001	<0.001

GGO, ground-glass opacity; EGFR, epidermal growth factor receptor; d, maximum tumor diameter; V, total tumor volume; CT, computed tomography.

EGFR mutation group and wild-type group significantly increased in the 2nd CT scans compared to the 1st ones (*Table 2*). Specifically, the diameter and volume of 75 lesions with mutant EGFR increased to 1.52±0.43 cm ( $P<0.001$ ) and 2.29±2.18 cm<sup>3</sup> ( $P<0.001$ ), respectively, while the diameter and volume of the 81 lesions with wild-type EGFR also increased to 1.39±0.46 cm ( $P<0.001$ ) and 1.88±1.94 cm<sup>3</sup> ( $P<0.001$ ), respectively (*Figure 2*). Finally, we concluded that in the first 2 CT scans, the growth ratio in EGFR-mutant GGOs (53±54)% was higher than wild-type GGOs' growth ratio (18±29)% ( $P<0.001$ ) (*Figure 2*).

To analyze the association between EGFR mutation status and growth of GGOs, we set a threshold value as an increase in total tumor volume of >50% during the periods between the two preoperative CT examinations. In the

second CT scans, 28 of 75 (37.3%) lesions in the EGFR mutation group were found to grow over 50% in volume compared to the 1st CT scans while there were only 9 in 81 (11.1%) lesions without mutation ( $\chi^2=14.8$ ,  $P<0.001$ ). Furthermore, we found no significantly robust increase ( $P=0.33$ ) in diameter of the 28 EGFR-mutant GGOs (0.37±0.14 cm) when compared to the 9 cases without EGFR mutation (0.28±0.12 cm) (*Table 3*). Growth ratio of volume between 28 mutant GGOs and 9 wild-type GGOs was consistent with the change of diameter [(108±48)% *vs.* (84±25)%,  $P=0.95$ ] (*Table 3*, *Figure 3*). Information on tumor growth of different EGFR genotype groups are presented in *Table 4*.

In the 1st CT scans, the proportions of mixed GGOs in the EGFR mutation group and the wild-type group are 68% (51 of 75) and 27% (22 of 81), respectively. The mean CTR



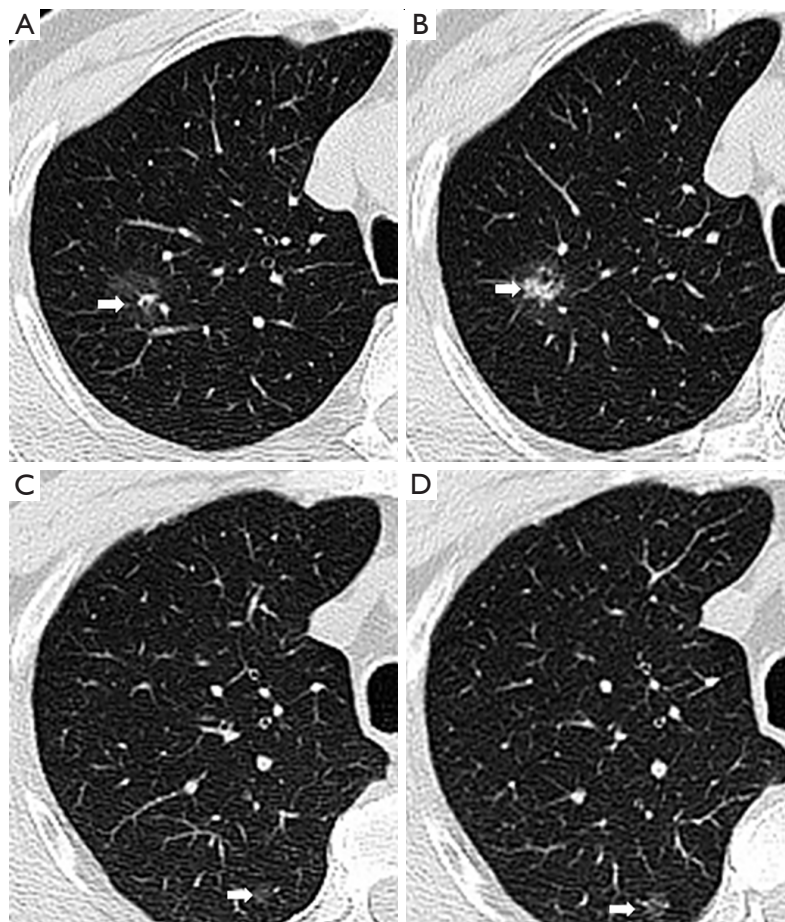


**Figure 1** Examples of increasing GGO or solid component of PSN with CT images. (A,B) The increment of solid part in a GGO (white arrow); (C,D) the volume increment of a GGO (white arrow). GGO, ground glass opacity; PSN, part solid-nodule.

in the 1st CT was 37.4% *vs.* 33.7% in EGFR mutation group and the wild-type group ( $P=0.61$ ). Solid proportion in pure GGOs or mixed GGOs was found increased in 38 of 75 (51%) and 14 of 81 (17%) GGOs in the EGFR mutation group and wild-type group, respectively ( $\chi^2=19.53$ ,  $P<0.001$ ) (Table 4). The mean CTR of 75 EGFR-mutant GGOs in 2nd CT was 41.2% *vs.* 35.4% in 81 EGFR-wild type GGOs ( $P=0.44$ ) while the mean CTR in the 38 EGFR-mutant SCI GGOs and 14 EGFR-wild type SCI GGOs were 46.9% and 38.3%, respectively ( $P=0.27$ ).

In order to figure out what is the potential relationship between EGFR mutation status and tumor recurrence, we reviewed the 3rd chest CT scans which were performed at  $213\pm90$  days after surgery ( $220\pm101$  days in EGFR mutation group and  $209\pm91$  days in wild-type group,  $P=0.85$ ). Six new pulmonary nodular opacities were found in both the EGFR mutation group and the wild-type group, which exhibited

no significant difference ( $\chi^2=0.02$ ,  $P=0.89$ ) (Table 4). As for the relationship between pathological type and tumor growth, we reached a conclusion that consolidation was more likely to happen in IA compared the other two types ( $\chi^2=6.27$ ,  $P=0.04$ ) (Table 5). Distribution of GGO volume percentages and estimated tumor diameters according to specific types of EGFR mutation are shown in Figure 4. We found that EGFR amplification is more frequent as GGO volume percentage decreases and diameter increases (Figure 5).

## Discussion

As one of the most aggressive human cancers, lung adenocarcinoma accounts for 40% of all the lung cancers and has a 5-year survival chance of 10–15% (19). Even for patients at the lowest stage of IA, 5-year overall

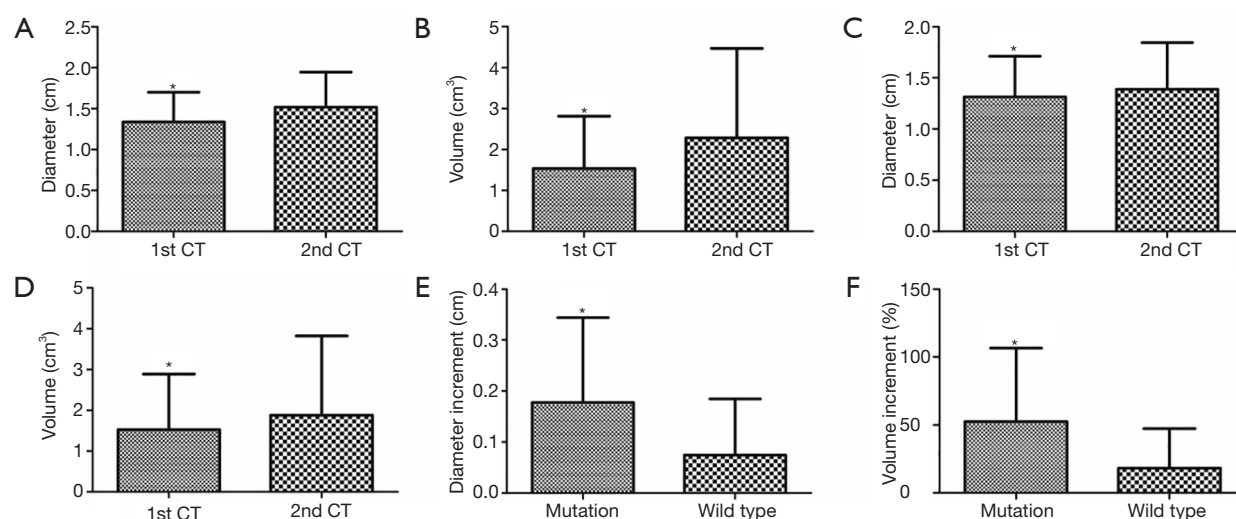


**Figure 2** The size comparison of GGOs between the 1st and 2nd chest CT. (A) The diameter of EGFR-mutant GGOs (n=75) in the 1st CT was significantly smaller than that in 2nd CT; (B) the volume of EGFR-mutant GGOs (n=75) in the 1st CT was significantly smaller than that in 2nd CT; (C) the diameter of wild-type GGOs (n=81) in the 1st CT was significantly smaller than that in 2nd CT; (D) the volume of wild-type GGOs (n=81) in the 1st CT was significantly smaller than that in 2nd CT; (E) diameter increment between 1st CT and 2nd CT in all GGOs (n=156); (F) volume increment (%) between 1st CT and 2nd CT in all GGOs (n=156). \*, P<0.05. GGO, ground glass opacity; EGFR, epidermal growth factor receptor; CT, computed tomography.

**Table 3** Diameter and volume increase of 28 VI GGOs in EGFR mutation group and 9 VI GGOs in wild-type group between 1st and 2nd chest CT scan

	$\Delta d$ (cm)	P	$\Delta V\%$	P
Mutation	$0.37 \pm 0.14$	0.33	$108 \pm 48$	0.95
Wild	$0.28 \pm 0.12$		$84 \pm 25$	

GGO, ground-glass opacity; EGFR, epidermal growth factor receptor; VI, volume increase  $\geq 50\%$ ; d, maximum tumor diameter; V, total tumor volume; CT, computed tomography.

survival is only approximately 50% (20). However, so far all cases reported as AIS and MIA have demonstrated 5-year disease-free survival of 100% after completely resected (21). Benefiting from advances in diagnostic modalities and widespread use of low-dose helical CT, more and more localized GGOs have been detected. Among these GGOs, most were pathologically proved as lung AAH, AIS or MIA and early-stage lung adenocarcinoma (2-4). Thus, it is of great importance to screen these patients and intervene as soon as possible.

Previous studies have reported that the GGOs, which pathologically proved adenocarcinoma at CT, correspond to a growth pattern involving alveolar septa lacking acinar filling (8). Gao *et al.* found EGFR amplification was negatively correlated with the GGO percentage, while the

frequency of FISH-positivity increased as the proportion of GGO decreased (1). A meta-analysis from Cheng *et al.* demonstrated that NSCLC with CT morphological features of part solid GGO tended to be EGFR mutated, which might provide an important clue for the correct selection of patients treated with molecular targeted therapies (5). Although the reason for consolidation of GGO lesions has not been elucidated, emergence and growth of solid portion is generally accepted as an advanced stage of GGO evolution, which augments the invasiveness of the tumor (22,23). Several studies reported a low proportion of the solid component as a good prognostic factor (5). The GGO proportion could be a good predictor of the histologic prognostic factors, and the GGO at CT in peripheral adenocarcinomas smaller than 3 cm, correlates with

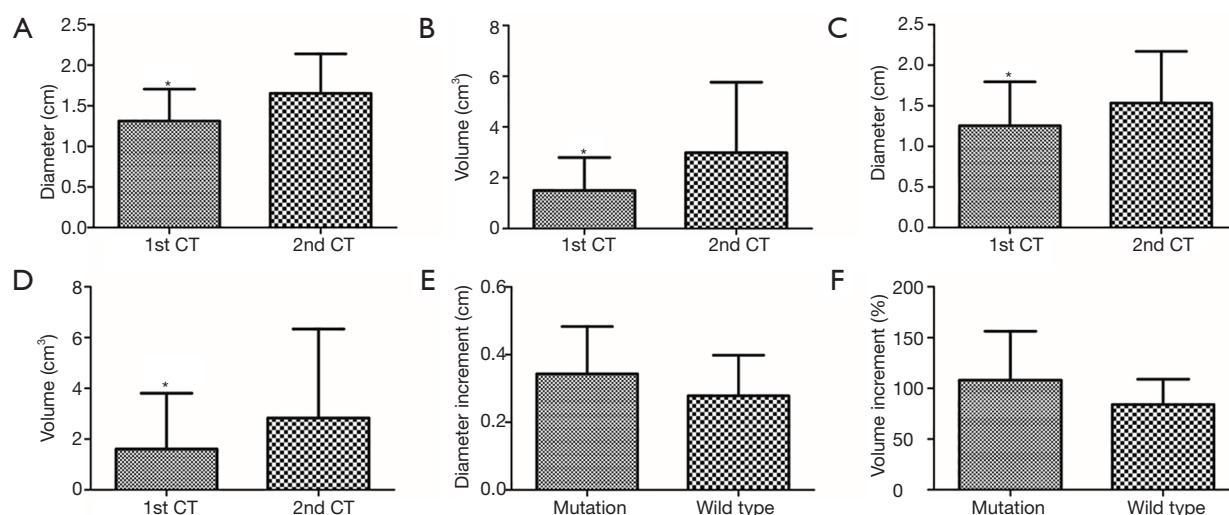


**Figure 3** The size comparison of GGOs between the 1st and 2nd chest CT. (A) The diameter of VI EGFR-mutant GGOs (n=28) in the 1st CT was significantly smaller than that in 2nd CT; (B) the volume of VI EGFR-mutant GGOs (n=28) in the 1st CT was significantly smaller than that in 2nd CT; (C) the diameter of VI wild-type GGOs (n=9) in the 1st CT was significantly smaller than that in 2nd CT; (D) the volume of VI wild-type GGOs (n=9) in the 1st CT was significantly smaller than that in 2nd CT; (E) diameter increment between 1st CT and 2nd CT in VI EGFR-mutant GGOs (n=28) and VI wild-type GGOs (n=9); (F) volume increment (%) between 1st CT and 2nd CT in VI EGFR-mutant GGOs (n=28) and VI wild-type GGOs (n=9). \*, P<0.05. VI, volume increase  $\geq 50\%$ . GGO, ground glass opacity; EGFR, epidermal growth factor receptor; CT, computed tomography.

**Table 4** The relationship between EGFR MS and RP in 156 patients presented as a solitary GGO

EGFR MS	n	VI		$\chi^2$	P	SCI		$\chi^2$	P	NFN		$\chi^2$	P
		+	-			+	-			+	-		
Mutation	75			14.8	<0.001			19.53	<0.001			0.02	0.89
Exon 18		0	1			0	1			0	1		
Exon 19		9	20			16	13			2	27		
Exon 21		19	26			22	23			4	41		
Wild	81	9	72			14	67			6	75		

GGO, ground glass opacity; EGFR, epidermal growth factor receptor; VI, volume increase  $\geq 50\%$ ; SCI, solid component increase; NFN, newly found node; RP, radiographic progression; MS, mutation status.

**Table 5** The relationship between pathology and tumor growth in 156 patients presenting as single GGO

Pathological status	VI		$\chi^2$	P	SCI		$\chi^2$	P	NFN		$\chi^2$	P
	+	-			+	-			+	-		
AAH/AIS	9	30	3.28	0.19	7	32	6.27	0.04	4	35	1.16	0.56
MIA	7	10			5	12			2	15		
IA	21	79			40	60			6	94		

GGO, ground glass opacity; EGFR, epidermal growth factor receptor; VI, volume increase  $\geq 50\%$ ; SCI, solid component increase; NFN, newly found node; AAH, atypical adenomatous hyperplasia; AIS, adenocarcinoma *in situ*; MIA, minimally invasive adenocarcinoma; IA, invasive adenocarcinoma.

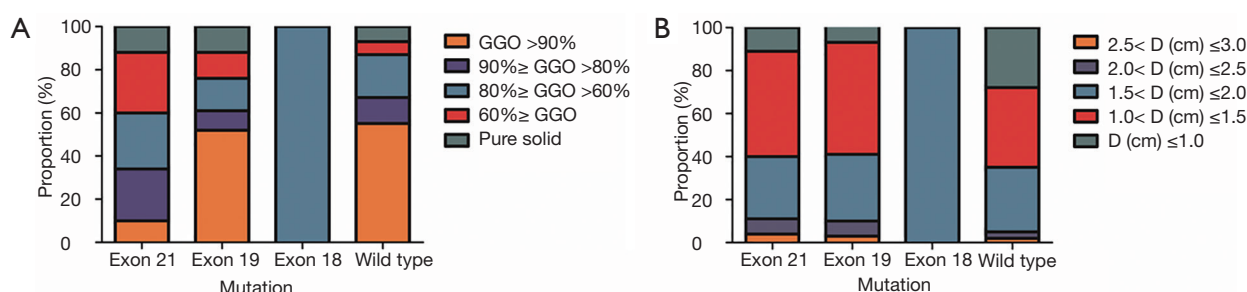


**Figure 4** Distribution of GGO volume percentages and estimated tumor diameters according to specific types of EGFR mutation. (A) Graph shows distribution of lung adenocarcinomas with different GGO volume percentages according to EGFR mutation status; (B) graph shows distribution of estimated tumor diameters according to EGFR mutation status. D, estimated tumor diameter. GGO, ground glass opacity; EGFR, epidermal growth factor receptor.

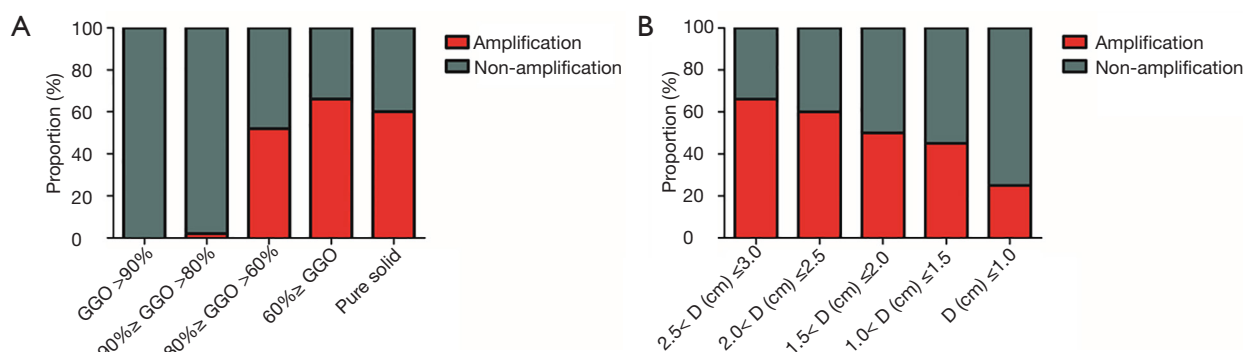


**Figure 5** Distribution of GGO volume percentages and estimated tumor diameters according to EGFR amplification. (A) Graph shows that EGFR amplification is more frequent as GGO volume percentage decreases; (B) graph shows that EGFR amplification is more often found as tumor diameter increases. D, estimated tumor diameter. GGO, ground glass opacity; EGFR, epidermal growth factor receptor.

favorable prognosis (24). The solid component within GGO lesions results from the invasive tumor growth, fibrosis, or a collapse of an alveolar space. If this process continues, it may lead to pleural indentation and/or vascular convergence of the surrounding area of the tumor (3). EGFR mutation was found correlated with many specific characteristics including nonsmokers, females, adenocarcinoma and East Asians; on the other hand, EGFR mutation indicates the increased sensitivity to EGFR-TKI (tyrosine kinase inhibitor) treatment (9). In Chinese, exon 19 deletion and exon 21 missense were more frequent in lepidic predominant adenocarcinomas (10). EGFR amplification has been reported to be associated with solid findings which was thought an indicator of an advanced stage in lung adenocarcinoma (20). Liu *et al.* concluded that CT imaging features of lung adenocarcinomas in combination with clinical variables can be used to prognosticate EGFR

mutation status better than use of clinical variables alone (7). Supposing that EGFR mutation status of lung cancer can be identified without molecular examination of EGFR mutation by biopsy or surgery, it might reduce aggravation to patients physically and financially.

In the present study, we analyzed the CT findings of patients with adenocarcinoma to identify some radiographic features that may predict the presence of EGFR mutations and the response to gefitinib. As a result, we found EGFR-mutant lesions grew more quickly than wild-type GGOs ( $P < 0.001$ ). Furthermore, the solid component in lesions with EGFR mutation increased faster compared to those lesions without EGFR mutation ( $P < 0.001$ ). Subsequently, in the follow-up after surgery, new GGOs or nodes were both found in the EGFR mutation group and the EGFR wild-type group ( $P = 0.89$ ). In addition, with the increase of solid proportion in GGO, AIS and MIA were shown to have a



decreasing trend, whereas IA exhibited an increasing trend.

These findings notwithstanding, there might still be several deficiencies in our study which need attention. First, the time in which the tumor doubles, is usually taken as an indicator in tumor growth; however, tumor doubling time for most lung cancers is between 30 and 400 days. Furthermore, previous studies have demonstrated that a dominant GGO at CT scan can double more slowly in adenocarcinoma (25). Another issue is that we considered volume increase (VI)  $\geq 50\%$  as a marker in our analysis because most patients were always anxious and were suggested to accept a surgery once the GGO was found larger than before. As such, we could not collect enough data to illustrate our views by using tumor doubling time. Second, most of our patients were diagnosed as IA, the shortage of AIS or MIA cases caused the uneven distribution of sample size of histologic subtypes. Third, we focused on patients presenting as single GGO, when actually a lot of patients were found with multiple GGOs in the same or different lobes. Finally, this is a single-center study, meaning the number of cases enrolled in this study was not large enough to make our conclusion more convincing, and the follow-up time was not long enough to monitor the prognosis of these patients.

## Conclusions

In conclusion, the high EGFR mutation rate could act as a promoter for the stimulation of GGO growth in lung adenocarcinoma. As of now, only by GGO biopsy or surgical resection can we tell the EGFR mutation status. Our study proposed a possibility to predict the EGFR mutation status by monitoring the chest CT evolvement in patients who come for help with GGO in their lungs, especially nonsmoking-females. It might become an indicator that a GGO could harbor the EGFR mutation and may have a good response to EGFR-TKI if it grows fast in a short period.

## Acknowledgements

We thank the staff from Department of Pathology in Changhai Hospital of Second Military Medical School (Shanghai, China) for the skillful technical support.

**Funding:** This study has received funding from the National Natural Science Foundation of China (Grant 81472688 and 81370355). Grant 81472688: The design of the study, data collection and analysis. Grant 81370355: The interpretation

of data and the writing of the manuscript.

## Footnote

**Conflicts of Interest:** The authors have no conflicts of interest to declare.

**Ethical Statement:** This study was approved by the Ethics Committee of the Changhai Hospital (No. CHEC2013-194), and the written informed consent was obtained from all participants with their medical record data anonymized prior to analysis.

## References

1. Gao JW, Rizzo S, Ma LH, et al. Pulmonary ground-glass opacity: computed tomography features, histopathology and molecular pathology. *Transl Lung Cancer Res* 2017;6:68-75.
2. Gu B, Burt BM, Merritt RE, et al. A dominant adenocarcinoma with multifocal ground glass lesions does not behave as advanced disease. *Ann Thorac Surg* 2013;96:411-8.
3. Aoki T, Hanamiya M, Uramoto H, et al. Adenocarcinomas with predominant ground-glass opacity: correlation of morphology and molecular biomarkers. *Radiology* 2012;264:590-6.
4. Matsuguma H, Oki I, Nakahara R, et al. Comparison of three measurements on computed tomography for the prediction of less invasiveness in patients with clinical stage I non-small cell lung cancer. *Ann Thorac Surg* 2013;95:1878-84.
5. Cheng Z, Shan F, Yang Y, et al. CT characteristics of non-small cell lung cancer with epidermal growth factor receptor mutation: a systematic review and meta-analysis. *BMC Med Imaging* 2017;17:5.
6. Liu M, He WX, Song N, et al. Discrepancy of epidermal growth factor receptor mutation in lung adenocarcinoma presenting as multiple ground-glass opacities. *Eur J Cardiothorac Surg* 2016;50:909-13.
7. Liu Y, Kim J, Qu F, et al. CT Features Associated with Epidermal Growth Factor Receptor Mutation Status in Patients with Lung Adenocarcinoma. *Radiology* 2016;280:271-80.
8. Noonan SA, Sachs PB, Camidge DR. Transient Asymptomatic Pulmonary Opacities Occurring during Osimertinib Treatment. *J Thorac Oncol* 2016;11:2253-8.
9. Zhou J, Ben S. Comparison of therapeutic effects of

- EGFR-tyrosine kinase inhibitors on 19Del and L858R mutations in advanced lung adenocarcinoma and effect on cellular immune function. *Thorac Cancer* 2018;9:228-33.
10. Ellison G, Zhu G, Moulis A, et al. EGFR mutation testing in lung cancer: a review of available methods and their use for analysis of tumour tissue and cytology samples. *J Clin Pathol* 2013;66:79-89.
  11. Liu M, He WX, Song N, et al. Discrepancy of epidermal growth factor receptor mutation in lung adenocarcinoma presenting as multiple ground-glass opacities. *Eur J Cardiothorac Surg* 2016;50:909-13.
  12. Cancer Genome Atlas Research Network. Comprehensive molecular profiling of lung adenocarcinoma. *Nature* 2014;511:543-50.
  13. Kobayashi Y, Mitsudomi T, Sakao Y, et al. Genetic features of pulmonary adenocarcinoma presenting with ground-glass nodules: the differences between nodules with and without growth. *Ann Oncol* 2015;26:156-61.
  14. Goldstraw P, Crowley J, Chansky K, et al. The IASLC Lung Cancer Staging Project: proposals for the revision of the TNM stage groupings in the forthcoming (seventh) edition of the TNM Classification of malignant tumours. *J Thorac Oncol* 2007;2:706-14.
  15. Travis WD, Brambilla E, Noguchi M, et al. International association for the study of lung cancer/american thoracic society/european respiratory society international multidisciplinary classification of lung adenocarcinoma. *J Thorac Oncol* 2011;6:244-85.
  16. Yang Y, Yang Y, Zhou X, et al. EGFR L858R mutation is associated with lung adenocarcinoma patients with dominant ground-glass opacity. *Lung Cancer* 2015;87:272-7.
  17. Zhang L, Yankelevitz DF, Henschke CI, et al. Zone of transition: a potential source of error in tumor volume estimation. *Radiology* 2010;256:633-9.
  18. Shimada Y, Saji H, Otani K, et al. Survival of a surgical series of lung cancer patients with synchronous multiple ground-glass opacities, and the management of their residual lesions. *Lung Cancer* 2015;88:174-80.
  19. Mariotto AB, Noone AM, Howlader N, et al. Cancer survival: an overview of measures, uses, and interpretation. *J Natl Cancer Inst Monogr* 2014;2014:145-86.
  20. Zou J, Lv T, Zhu S, et al. Computed tomography and clinical features associated with epidermal growth factor receptor mutation status in stage I/II lung adenocarcinoma. *Thorac Cancer* 2017;8:260-70.
  21. Travis WD, Brambilla E, Riely GJ. New pathologic classification of lung cancer: relevance for clinical practice and clinical trials. *J Clin Oncol* 2013;31:992-1001.
  22. Wang T, Zhang T, Han X, et al. Impact of the International Association for the Study of Lung Cancer/American Thoracic Society/European Respiratory Society classification of stage IA adenocarcinoma of the lung: Correlation between computed tomography images and EGFR and KRAS gene mutations. *Exp Ther Med* 2015;9:2095-103.
  23. Zhou JY, Zheng J, Yu ZF, et al. Comparative analysis of clinicoradiologic characteristics of lung adenocarcinomas with ALK rearrangements or EGFR mutations. *Eur Radiol* 2015;25:1257-66.
  24. Zhong WZ, Wang Q, Mao WM, et al. Gefitinib versus vinorelbine plus cisplatin as adjuvant treatment for stage II-IIIa (N1-N2) EGFR-mutant NSCLC (ADJUVANT/CTONG1104): a randomised, open-label, phase 3 study. *Lancet Oncol* 2018;19:139-48.
  25. Sagawa M, Oizumi H, Suzuki H, et al. A prospective 5-year follow-up study after limited resection for lung cancer with ground-glass opacity. *Eur J Cardiothorac Surg* 2018;53:849-56.

**Cite this article as:** Lu Q, Ma Y, An Z, Zhao T, Xu Z, Chen H. Epidermal growth factor receptor mutation accelerates radiographic progression in lung adenocarcinoma presented as a solitary ground-glass opacity. *J Thorac Dis* 2018;10(11):6030-6039. doi: 10.21037/jtd.2018.10.19